

# Phys4DGen: A Physics-Driven Framework for Controllable and Efficient 4D Content Generation from a Single Image

Jiajing Lin Zhenzhong Wang Shu Jiang Yongjie Hou Min Jiang\*  
School of Informatics, Xiamen University

## Abstract

The task of 4D content generation involves creating dynamic 3D models that evolve over time in response to specific input conditions, such as images. Existing methods rely heavily on pre-trained video diffusion models to guide 4D content dynamics, but these approaches often fail to capture essential physical principles, as video diffusion models lack a robust understanding of real-world physics. Moreover, these models face challenges in providing fine-grained control over dynamics and exhibit high computational costs. In this work, we propose Phys4DGen, a novel, high-efficiency framework that generates physics-compliant 4D content from a single image with enhanced control capabilities. Our approach uniquely integrates physical simulations into the 4D generation pipeline, ensuring adherence to fundamental physical laws. Inspired by the human ability to infer physical properties visually, we introduce a Physical Perception Module (PPM) that discerns the material properties and structural components of the 3D object from the input image, facilitating accurate downstream simulations. Phys4DGen significantly accelerates the 4D generation process by eliminating iterative optimization steps in the dynamics modeling phase. It allows users to intuitively control the movement speed and direction of generated 4D content by adjusting external forces, achieving finely tunable, physically plausible animations. Extensive evaluations show that Phys4DGen outperforms existing methods in both inference speed and physical realism, producing high-quality, controllable 4D content.

## 1. Introduction

The generation of 4D content is becoming increasingly valuable in a variety of fields, such as animation, gaming, and virtual reality [3]. Recent advancements in diffusion models [10] have revolutionized image generation [24, 37] and video generation [4, 30]. These models' robust visual priors have significantly propelled progress in 4D content

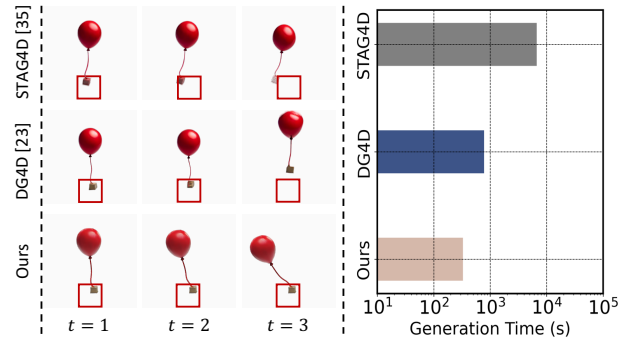


Figure 1. The figure shows a balloon tied to a wooden block sways in the wind. The red box is used as a reference point to help with observation. STAG4D and DG4D struggle to generate dynamics that are both physically realistic and meet user requirements. For example, the motion of the balloon shown in the figure violates the laws of gravity. In contrast, our approach can generate 4D content with greater physical accuracy. Moreover, our method reduces the generation time to 42% of the time taken by DG4D.

generation [2, 39]. Such progress has made the automated production of high-quality 4D content not only achievable but also increasingly efficient.

Generating 4D content from a single image presents a formidable challenge due to the inherent absence of both temporal and spatial information in a single image. Unlike image-to-3D generation, which focuses on spatially consistent shapes and appearances, image-to-4D generation prioritizes the creation of realistic and temporally consistent 4D dynamics. Existing methods [16, 23, 34, 35, 39] predominantly rely on pre-trained video diffusion models to capture dynamic information. Animate124 [39] is a pioneering framework that adopts temporal score distillation sampling (SDS) from a video diffusion model to optimize 4D dynamics. However, Animate124 struggles to converge and has difficulty generating 4D content that aligns with the input images. To improve the efficiency and quality of generation, DreamGaussian4D [23] employs deformable 3D Gaussians [32] as 4D representations. It generates reference videos through a video diffusion model to determine the 4D

\*Corresponding author

dynamics. Subsequently, supervised loss and SDS from the 3D aware diffusion model is used to refine the 4D representation to match the reference video. To further enhance spatial and temporal consistency, some methods [16, 27, 35] use diffusion models to pre-generate image sequences from multiple viewpoints of the reference video, offering richer reference information for optimization.

Despite these advancements, existing methods still face several critical challenges. Firstly, the reliance on video diffusion models, which often fail to effectively learn physical principles, results in 4D content that frequently violates physical laws, as illustrated in the left part of Fig. 1. Secondly, the large scale of iterative optimization results in excessively time-consuming generation processes, as shown in the right part of Fig. 1. Additionally, the inherently stochastic nature of video diffusion models often leads to uncontrollable dynamics within the generated 4D content.

To address these challenges, we introduce *Phys4DGen*, a physics-driven method capable of generating controllable 4D content from a single image. Our key insight is the integration of physical simulation into the 4D generation process. To achieve this, we first generate static Gaussians. Since physical simulation requires predefined physical properties, such as material types and attributes, we propose a Physical Perception Module (PPM) to accurately predict these properties for different components of the 3D objects described in the images. Finally, using the predicted physical properties and applying external forces, we perform the physical simulation to generate the 4D content.

Unlike most current methods [16, 23, 27, 39] that rely on video diffusion models to determine dynamics in 4D content, *Phys4DGen* applies physical simulation to ensure that the generated 4D content adheres to physical laws. In previous methods [31], 3D objects were typically treated as a whole, with the same material types and properties manually assigned for simulation. In this paper, we use PPM to automatically segment materials and assign the corresponding material types and properties, enabling more accurate and realistic simulations. Moreover, by eliminating the large iterative optimization steps during the 4D dynamics generation phase, *Phys4DGen* achieves rapid 4D content generation from a single image. To provide fine-grained control over the dynamics in the generated 4D content, we introduce external forces. By fine-tuning these external forces, *Phys4DGen* can generate 4D content that aligns with user intent. The main contributions of our work are summarized as follows:

- We present a physics-driven image-to-4D generation framework that integrates physical simulation seamlessly into the 4D generation process, enabling the rapid and fine-grained controllable production of 4D content that adheres to physical principles.
- We first propose a Physical Perception Module (PPM) to

infer the material types and properties of various components in 3D objects from input images, enabling accurate downstream simulations.

Qualitative and quantitative comparisons demonstrate that our method generates 4D content that is physically accurate, spatially and temporally consistent, high-fidelity, and controllable, with significantly reduced generation times.

## 2. Related Work

### 2.1. 4D Generation

4D generation [9, 19, 40] aims to generate dynamic 3D content that aligns with input conditions such as text, images, and videos. Currently, most 4D generation work [2, 7, 12, 34, 39] heavily depends on diffusion models [26]. Based on the input conditions, 4D generation can be categorized into three types: text-to-4D, video-to-4D, and image-to-4D. For instance, MAV3D [25] is the first text-to-4D work that trains HexPlane [6] using temporal SDS from a text-to-video diffusion model. 4D-fy [2] tackles the text-to-4D task by integrating various diffusion priors. However, these methods all suffer from time-consuming optimization. Instead of text input, Consistent4D [12] is an approach for generating 360-degree dynamic objects from monocular video by introducing cascade DyNeRF and interpolation-driven consistency loss. 4DGen [34] supervised using pseudo labels generated by a multi-view diffusion model. In practice, acquiring high-quality reference videos can be challenging. Animate124 [39] pioneered an image-to-4D framework using a coarse-to-fine strategy that combines different diffusion priors. However, Animate124 struggles to generate 4D content that accurately matches the input image (see Fig. 1). The process of generating 4D content from an image in DreamGaussian4D [23] avoids using temporal SDS and instead performs optimization based on reference videos generated by a video diffusion model. Yet, generating high-quality reference videos with video diffusion models is often challenging. Compared to previous works, our framework can efficiently generate 4D content from a single image, avoiding the time-consuming optimization process during 4D dynamics generation phase, and enabling high-fidelity and controllable 4D generation.

### 2.2. Physical Simulation

The explicit representation of 3D Gaussian Splatting (3DGS) [13] through a set of anisotropic Gaussian kernels, which can be interpreted as particles in space, enables the many application of physical simulations [5, 8, 31, 41] [31] is the first study to apply physical simulation to a given static 3D Gaussian for simulating realistic dynamic effects. Subsequently, several works combining 3DGS with physics simulations have gradually emerged. [38] utilizes refer-

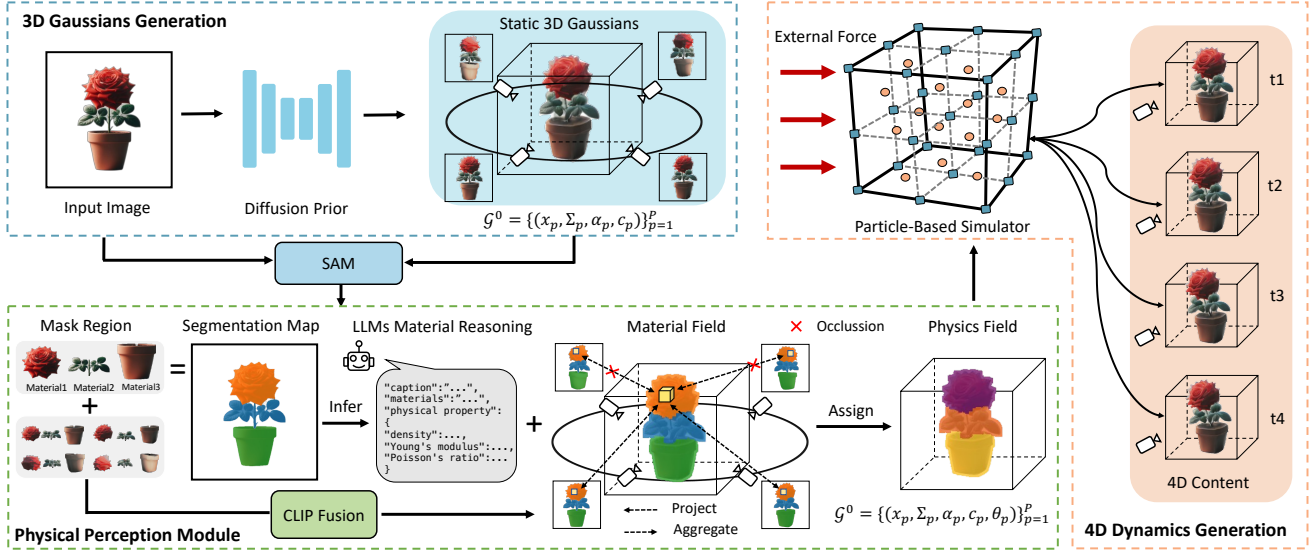


Figure 2. **Framework of Phys4DGen.** In **3D Gaussians Generation** stage, from an input image, a static 3D Gaussians will be generated under the guidance of the diffusion model. In **Physical Perception** stage, the 3D Gaussians will be segmented into different parts, with corresponding material types and properties assigned to each. In **4D Dynamics Generation** stage, we consider each 3D Gaussian kernel as particles within a continuum. Sequentially, we employ MPM to generate dynamics to the static 3D Gaussians. Meanwhile, users can guide the MPM simulator to generate 4D content that aligns with their desired outcomes by adjusting the external forces.

ence videos from video diffusion models for supervision to autonomously determine material property values. In contrast, [11, 17] uses score distillation sampling from video diffusion models to optimize physical properties. [21] explores incorporating 3D perception to autonomously identify specific parts within a space, and then edit or simulate those parts. The aforementioned research has promoted the combination of 3DGS and physics simulation.

### 2.3. 3D Perception

3D perception is crucial for robotics, autonomous driving, and physical simulation. With the significant progress in 2D scene understanding achieved by SAM [15], recent studies [14, 20, 33, 42] have attempted to distill the prior knowledge of 2D perception to achieve 3D perception. LERF [14] is the first to embed CLIP features [22] into NeRF [18], enabling open-vocabulary 3D queries. However, due to the NeRF-based representation approach, LERF suffers from significant limitations in speed. Recently, more work has focused on integrating 2D perception priors with 3D Gaussians to create a real-time, editable 3D scene representation. LangSplat [20] introduces hierarchical semantics—subparts, parts, and wholes—constructed using SAM, which addresses point ambiguity and facilitates scene understanding. Gaussian Grouping [33] introduces the concept of Gaussian groups and assigns an identity encoding to each Gaussian kernel to identify its respective Gaussian group, to achieve better editing. However, these methods

are unable to perceive the physical characteristics. Recently, [36] have attempted to integrate NeRF with large language models to predict the physical properties of objects. However, due to the inability to accurately distinguish between different materials, the predictions are often imprecise. In this work, we propose a Physical Perception Module (PPM) to accurately perceive the physical characteristics of different components of the 3D objects.

## 3. Methodology

The proposed *Phys4DGen* is illustrated in Fig 2. The framework includes three phases: **3D Gaussians Generation**, **Physical Perception**, and **4D Dynamics Generation**. In **3D Gaussians Generation**, a static 3D Gaussians is generated from an input image under the guidance of the image diffusion model. Sequentially, in **Physical Perception**, given an input image and static 3D Gaussians, we utilize the PPM to infer and assign material types and properties to different parts of static 3D Gaussians. Finally, in **4D Dynamics Generation**, given external forces, dynamics are generated from static 3D Gaussians with physical properties through physical simulation. Specifically, *Phys4DGen* enables the control of 4D dynamics, including movement speed and direction, by manipulating external forces. In the following parts, we provide details of **3D Gaussians Generation**, **Physical Perception** and **4D Dynamics Generation**.

### 3.1. 3D Gaussians Generation

For 3D Gaussians generation, static 3D Gaussians can be generated from a single image using any image-to-3D generation method [28, 29] based 3DGS, providing plug-and-play capability. Additionally, the quality of the 4D content improves with the quality of the static 3D Gaussians generated from the input image. We choose 3DGS for its explicit representation nature. 3DGS represents 3D objects using a collection of anisotropic Gaussian kernels [13], which can be interpreted as particles in space. Thus, 3D Gaussians can be viewed as a discretization of the continuum, which is highly beneficial for integrating particle-based physical simulation algorithms. In this phase, we obtain a static 3D Gaussians  $\mathcal{G}^0 = \{(\mathbf{x}_p, \Sigma_p, \alpha_p, \mathbf{c}_p)\}_{p=1}^P$  for subsequent simulation. Here,  $\mathbf{x}_p$ ,  $\Sigma_p$ ,  $\alpha_p$ , and  $\mathbf{c}_p$  represent the center position, covariance matrix, opacity, and color of the Gaussian kernel  $p$ , respectively, and  $P$  denotes the total number of Gaussian kernels in the 3D Gaussians.

### 3.2. Physical Perception

Physical simulation based on 3DGS requires predefined physical properties, such as material types and properties, for the Gaussian kernels representing the simulation objects. In practical applications, these objects typically consist of components with varying physical properties. However, previous studies [31] typically treat the simulation object as a single material type, with manually assigned properties, often resulting in imprecise simulation outcomes. In this section, we propose PPM. Our core idea is to integrate large vision and language models to first segment the simulation object into multiple material parts, and then infer the material type and properties of each part. The specific process is shown in Fig. 2.

#### 3.2.1. Material Segmentation

In practice, objects are usually made up of various materials. Accurately predicting the physical properties of different parts of a 3D object first requires precise segmentation of its materials. Specifically, we need to assign a material group  $E^{id}$  to each Gaussian kernel. The user-specified input image contains richer and more accurate semantic information than rendered images. Thus, we define material groups based on the segmentation results of the input image, ensuring that each mask region corresponds to a specific material group. We propose a material segmentation method that assigns material groups from the input image to corresponding Gaussian kernels.

**Pre-process.** For **3D Gaussians generation**, we generate a static 3D Gaussians from input image  $I_0$ , then render images and depth from  $N$  given viewpoints to produce image sequence  $\mathcal{I} = \{I_o\}_{o=1}^N$ . SAM [15] is a powerful foundation model for image segmentation that can accurately group pixels with surrounding pixels belonging to the same

part. Given SAM’s ability to distinguish various materials, we use it to segment both the input image and the rendered sequence, obtaining the segmentation map  $\mathbf{M}_0$  for the input image and  $\{\mathbf{M}_o\}_{o=1}^N$  for the rendered sequence.

**CLIP Fusion.** However, the 2D segmentation maps are generated independently, lacking connections between the maps of different images. To ensure consistency with the material groups defined by the input image, we align the segmentation maps  $\{\mathbf{M}_o\}_{o=1}^N$  of the rendered sequence with the input image’s segmentation map  $\mathbf{M}_0$ . Specifically, we first extract the CLIP features for all mask regions in the input image and the rendered image sequence, represented as:

$$\mathbf{L}_0(m) = \mathbf{V}(I_0 \odot \mathbf{M}_0(m)), \quad (1)$$

$$\mathbf{L}_o(k) = \mathbf{V}(I_o \odot \mathbf{M}_o(k)), \quad (2)$$

where  $\mathbf{V}$  is the CLIP image encoder and  $\mathbf{L}$  represents the mask CLIP embedding.  $\mathbf{M}(k)$  denotes the  $k$ -th mask region in the specified segmentation map, where different maps may contain varying numbers of mask regions. Next, we calculate the similarity between the mask CLIP features of the input image and those of the rendered sequence. We then update the segmentation map for each rendered image, assigning each region the material group with the highest CLIP similarity score. This process is mathematically represented as follows:

$$\mathbf{M}_o(k) = \arg \max \{\mathbf{L}_o(k) \cdot \mathbf{L}_0(m)\}_m^{\mathcal{M}}, \quad (3)$$

where  $\mathcal{M}$  represents the total material groups. In this way, we align the segmentation maps of the rendered sequence with the segmentation map of the input image.

**Projection and Aggregation.** At this stage, we have a sequence of segmentation maps with consistent material groupings, and we need to assign a material group to each Gaussian kernel. For a random Gaussian kernel  $\mathcal{G}_p^0$  and a segmentation map  $\mathbf{M}_o$ , we use the camera’s intrinsic and extrinsic parameters to project the Gaussian kernel into 2D space, obtaining the 2D coordinates  $\mathbf{x}_p^{2d}$  on the segmentation map. This process can be expressed as:

$$\mathbf{x}_p^{2d} = \mathbf{K}[\mathbf{R}_o | \mathbf{T}_o] \mathbf{x}_p, \quad (4)$$

where  $\mathbf{K}$  and  $[\mathbf{R}_o | \mathbf{T}_o]$  represent the camera’s intrinsic and extrinsic parameters, respectively. We use the 3DGS-estimated depth to check if the Gaussian kernel is visible in the segmentation map  $\mathbf{M}_o$ . After processing the segmentation maps for all viewpoints, we assign the material group that appears most frequently across all views to each Gaussian kernel. Repeating these steps allows us to determine the material groups for all Gaussian kernels  $\mathcal{G}^0 = (\mathbf{x}_p, \Sigma_p, \alpha_p, \mathbf{c}_p, E_p^{id})_{p=1}^P$ .

### 3.2.2. Material Reasoning

There is a wide variety of materials in the world, yet humans can infer their physical properties visually based on past experience. In recent years, large language models have advanced rapidly, incorporating extensive textual and multimodal knowledge and exhibiting reasoning abilities that approach or even surpass human-level understanding. Inspired by this, we leverage GPT-4o [1] for open-vocabulary semantic reasoning about material properties, including types and characteristics.

In Material Segmentation, each Gaussian kernel is assigned a material group based on the input image, where mask regions correspond directly to specific material groups. We extract sub-images from the input image according to these mask regions, which can be expressed as  $I_0 \odot M_0(m)_m^M$ . Following this, we pass both the full input image and the segmented sub-images into GPT-4, prompting it to reason the material type and properties for the material described in each segmented sub-images. Detailed prompts will be provided in the appendix. Since the segmented sub-images correspond one-to-one with the material groups, we can assign the inference results to each Gaussian kernel based on these groups, resulting in a material field represented by Gaussian kernels, denoted as  $\mathcal{G}^0 = (\mathbf{x}_p, \Sigma_p, \alpha_p, \mathbf{c}_p, \theta_p)_{p=1}^P$ .

This method assigns different material types to each Gaussian kernel in space, enabling more detailed and realistic simulations. In traditional physical simulation workflows, physical properties are typically set manually by users. However, in 4D generation, users often lack expertise in physics. This approach provides users with relatively accurate reference values for material properties, assisting in the creation of 4D content.

### 3.3. 4D Dynamics Generation

In this work, we introduce physical simulation to drive the dynamics generation. In this part, we briefly introduce the concept of external forces. Then, we present the details of how physical simulation is integrated into our framework.

#### 3.3.1. External Forces.

In physical simulations, external forces directly affect the system’s behavior. These forces, such as gravity, influence a continuum’s motion and deformation. In this paper, we apply two types of external forces. The first type directly modifies the particle’s velocity, such as setting the velocity of all particles to simulate the translation of the continuum. The second type indirectly affects the particle’s velocity by applying forces  $\mathbf{f}$ . For example, gravity can simulate the continuum’s fall. Given a force  $\mathbf{f}$ , we apply Newton’s second law and time integration to compute the particle’s ve-

locity at the next time step:

$$\mathbf{a}_p^t = \frac{\mathbf{f}}{m_p^t}, \quad \mathbf{v}_p^{t+1} = \mathbf{v}_p^t + \mathbf{a}_p^t \Delta t, \quad (5)$$

where  $\mathbf{a}_p^t$  denotes the acceleration of particle  $p$  at time step  $t$ , and  $\Delta t$  denotes the time interval between time step  $t$  and  $t + 1$ . By adjusting the external forces, we can control the motion and deformation of the object.

#### 3.3.2. Dynamics Generation.

*Phys4DGen* can integrate any particle-based physical simulation algorithm. In this paper, we use the Material Point Method (MPM) to simulate the dynamics of 4D content. For the detailed implementation of MPM, please refer to the appendix. Particularly, 3D Gaussians can be viewed as a discretization of the continuum, making it straightforward to integrate MPM. Therefore, we treat each Gaussian kernel as a particle in the continuum and endow each Gaussian kernel with time property  $t$  and physical properties  $\theta$ . Therefore, each Gaussian kernel can be expressed as:

$$\mathcal{G}_p^t = (\mathbf{x}_p^t, \Sigma_p^t, \sigma_p, \mathbf{c}_p, \theta_p^t). \quad (6)$$

Here, the subscript  $p$  denotes a specific Gaussian kernel within the continuum. Following [31], we employ MPM to perform physical simulations on the continuum represented by 3D Gaussian Splatting (3DGS). This allows us to track the position and shape changes of each Gaussian kernel at every time step:

$$\mathbf{x}^{t+1}, \mathbf{F}^{t+1}, \mathbf{v}^{t+1} = \text{MPMSimulation}(\mathcal{G}^t), \quad (7)$$

where  $\mathbf{x}^{t+1} = \{\mathbf{x}_p^{t+1}\}_{p=1}^P$  denotes the positions of all Gaussian kernel at time step  $t + 1$ .  $\mathbf{F}^{t+1} = \{\mathbf{F}_p^{t+1}\}_{p=1}^P$  represents deformation gradients, which describe the local deformation of each Gaussian kernel at time step  $t + 1$ . Intuitively, we can consider the deformation gradient as a local affine transformation applied to the Gaussian kernel. Consequently, we can derive the covariance matrix of Gaussian kernel  $p$  in step  $t + 1$ :

$$\Sigma_p^{t+1} = (\mathbf{F}_p^{t+1}) \Sigma_p^t (\mathbf{F}_p^{t+1})^T. \quad (8)$$

At each MPM simulation step, we obtain the motion and deformation information of the continuum represented by static 3D Gaussians.

This allows us to generate 4D dynamics that are consistent with physical constraints. At this phase, we have entirely eliminated the need for iterative optimization, which significantly speeds up the generation of 4D content. By controlling external forces, we can precisely manage the dynamics of 4D content generated from a single image, making our method highly controllable.

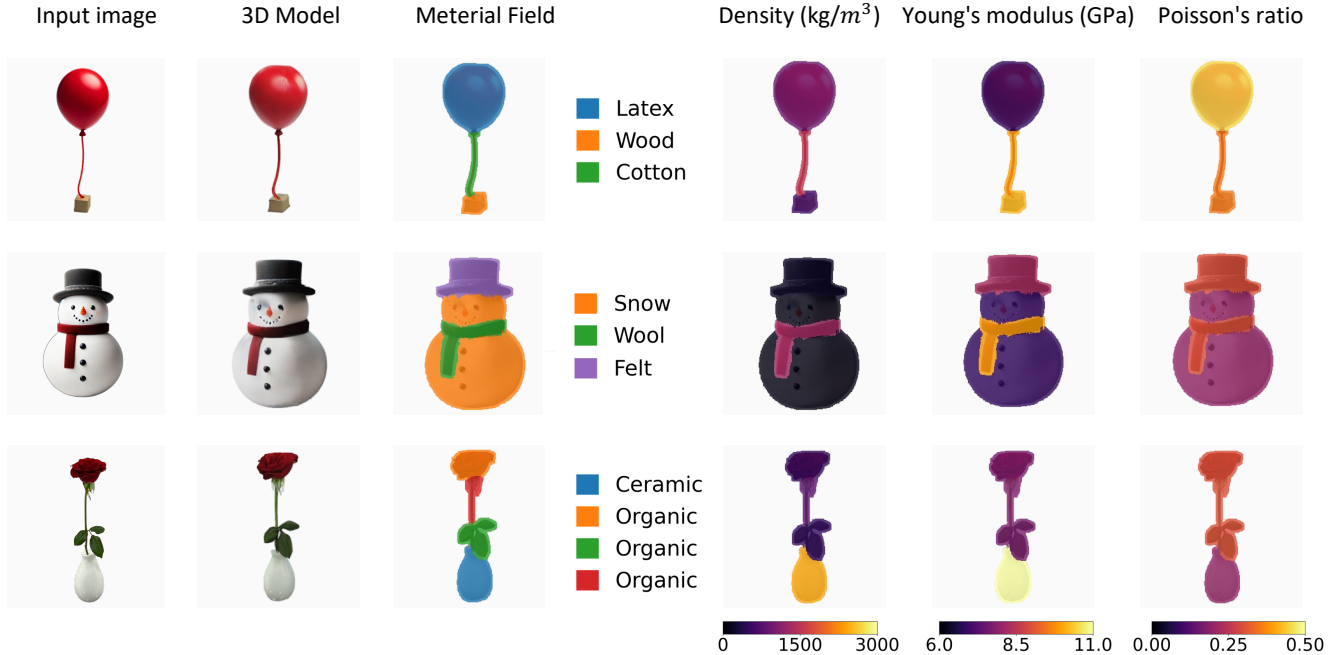


Figure 3. **Perception Visualization.** PPM can assign the appropriate material types and properties to the different parts of the objects.

## 4. Experiments

### 4.1. Experimental Setup

*Phys4DGen* is compared with current state-of-the-art (SOTA) approaches, including the STAG4D [35] and the DG4D [23]. Following [39], we conducted qualitative and quantitative evaluations to demonstrate the effectiveness of our method. For the quantitative evaluation, we used CLIP-T scores. CLIP-T score calculates the average cosine similarity between the CLIP embeddings of every two adjacent frames in rendered video from a given view. We use LGM [29] to generate static 3D Gaussians, with LGM settings consistent with those in the original implementation. We use the LangSplat [20] implementation to obtain part-level masks and adopt SAM ViT-H [15] as the base segmentation model. To infer physical properties, we use the GPT-4 language model, with specific prompts provided in the appendix. For the 4D dynamics generation phase, we employ MPM to generate dynamics, with the MPM settings following those in [31]. All experiments are performed on NVIDIA A40(48GB) GPU. For more detailed information on experimental settings, please refer to the appendix.

### 4.2. Comparisons with State-of-the-Art Methods

**Qualitative Results.** The results of the perception visualization, presented in the appendix, demonstrate that PPM effectively segments materials and assigns material types and properties. Fig. 4 shows the qualitative comparison between our method and other SOTA methods. To compare

Method	STAG4D	DG4D	Ours
CLIP-T- <i>f</i> ↑	0.9874	0.9922	<b>0.9956</b>
CLIP-T- <i>r</i> ↑	0.9833	0.9877	<b>0.9926</b>
CLIP-T- <i>b</i> ↑	0.9831	0.9890	<b>0.9938</b>
CLIP-T- <i>l</i> ↑	0.9845	0.9839	<b>0.9968</b>
Time ↓	6668s	780s	<b>330s</b>

Table 1. Quantitative comparison with other methods in terms of video quality and generation time. The notations *f*, *r*, *b*, and *l* denote the front, right, back, and left rendered views, respectively.

the spatiotemporal consistency, the rendering view changes with each time step. The text description below the input image specifies the desired dynamic effect. For example, a snowman is melting. Fig. 4 clearly demonstrates that our generated 4D content achieves high fidelity and excellent spatiotemporal consistency, significantly outperforming the baseline methods. The results show that *Phys4DGen* can generate 4D content that follows physical laws and provides fine-grained controllability. The process of generating 4D content with STAG4D and DG4D heavily depends on the quality of the reference video. However, it is challenging to obtain a reference video from existing video diffusion models that adhere to physical laws. As shown in Fig. 4, the 4D content generated by STAG4D and DG4D is hard to control and inconsistent with physical laws.

**Quantitative Results.** Table 1 presents a quantitative comparison between our method and other approaches. We

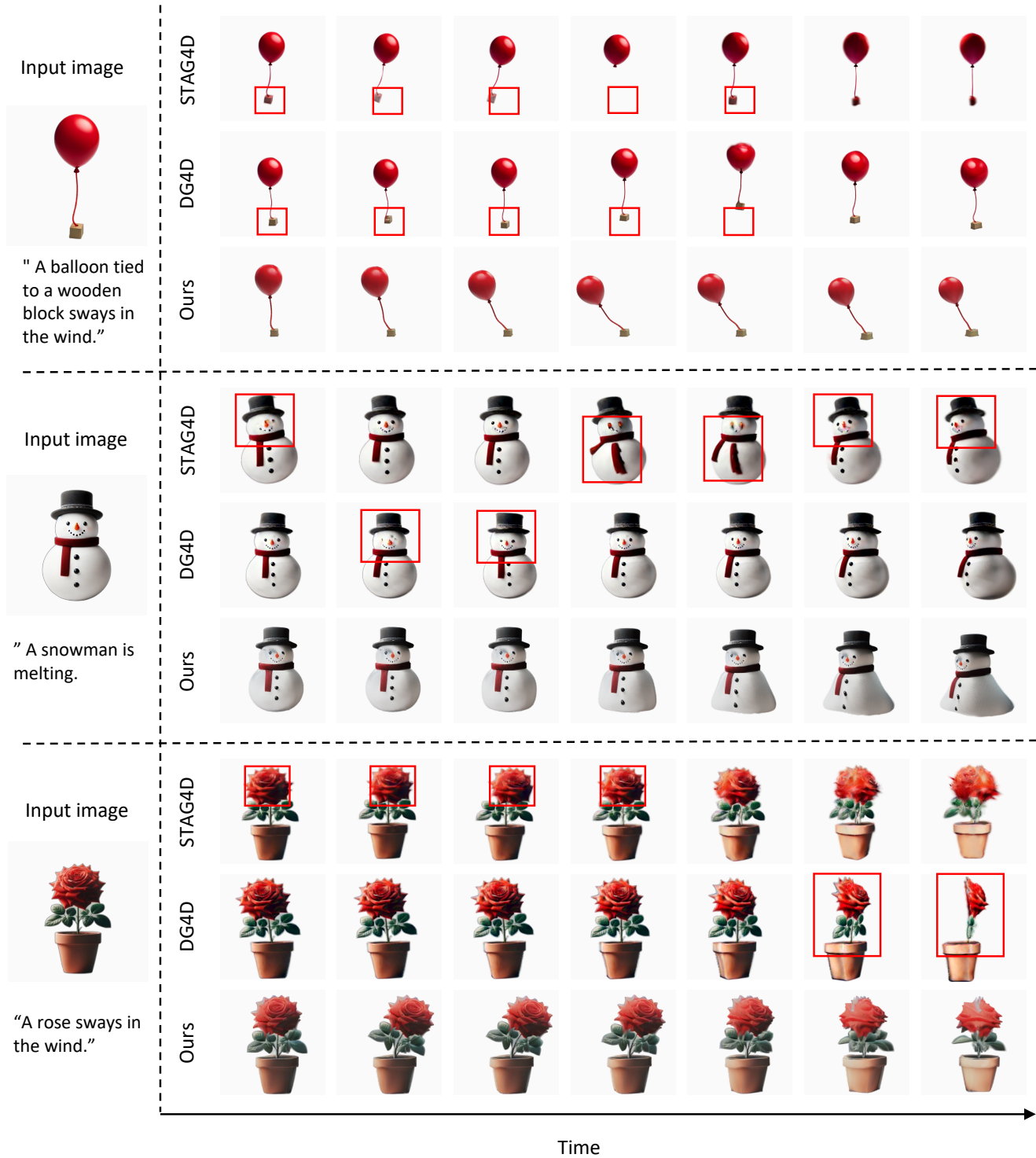


Figure 4. **Qualitative comparison with the baseline methods for image-to-4D generation.** The description below the input image outlines the 4D content the user aims to generate. The red box indicates the dynamics that violate physical laws. For each method, 14 frames of 4D content are generated, and every second frame is selected for display, showing a total of seven frames. Additionally, to compare spatial and temporal consistency across multiple views, the rendering perspective will change with each time step.

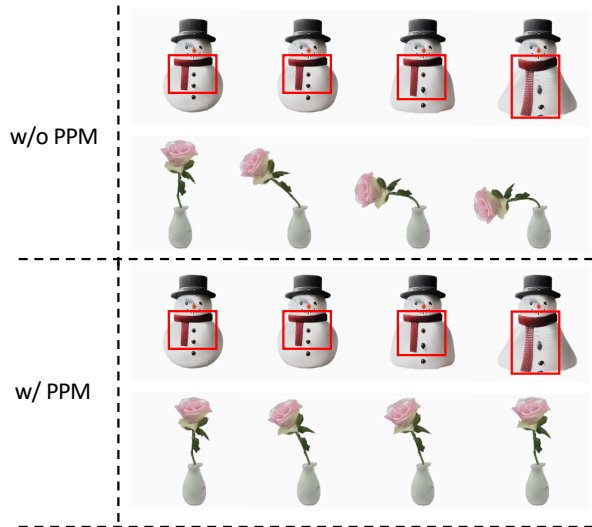


Figure 5. **Physical Perception Module Analysis.** PPM enables the generation of more physically realistic 4D content.

evaluate video quality using the CLIP-T score [22] and generation time. To further quantify spatiotemporal consistency, we rendered videos from the front, right, back, and left views and computed the CLIP-T score for each view. Table 1 shows that our approach outperforms the baseline methods on all metrics. This demonstrates that *Phys4DGen* generates 4D content that adheres to physical laws and ensures spatiotemporal consistency. Meanwhile, *Phys4DGen* generates 4D content in just 330 seconds, significantly reducing the time compared to the baseline methods.

### 4.3. Ablation Studies and Analysis

**The Effectiveness of Physical Perception Module.** In Fig. 5, we analyze the impact of incorporating the Physical Perception Module on the generation of 4D content. Firstly, as shown in the snowman example in Fig. 5, when PPM is not used to assign distinct material types to different parts of the snowman, the simulation algorithm treats the snowman as a uniform object, simulating the melting effect across the entire structure. As seen in Fig. 5, the scarf melts along with the snowman’s body, which clearly contradicts physical reality. PPM accurately segments materials and assigns their respective material types, thereby enabling more precise simulations. Secondly, as demonstrated by the pink rose in Fig. 5, when randomly generated material property values are used, the results lack physical realism. Users in the 4D generation often lack specialized knowledge of physics, making it challenging to assign material properties accurately. PPM automates the assignment of realistic property values to materials, enabling users to achieve more autonomous and physically consistent 4D generation.

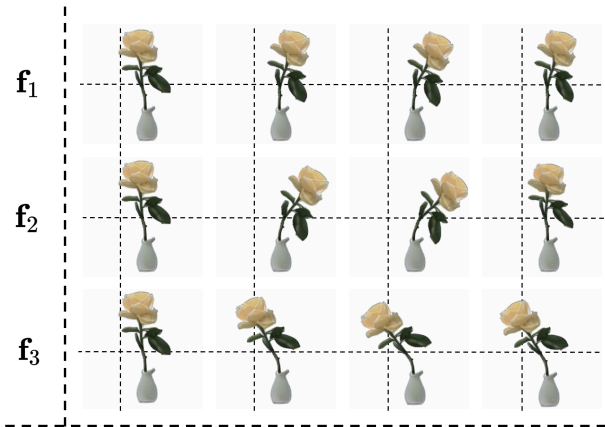


Figure 6. **External Forces Analysis.** 4D content is generated by applying different external forces  $f$ .

### The Ability for Fine-grained Controlling 4D Dynamics.

Fig. 6 illustrates the 4D content generated under various external forces, showcasing the fine-grained controllability of *Phys4DGen*. In the first row, external force  $f_1 = (1.0, 0.0, 0.0)$ , directed to the right along the x-axis is applied, causing the orange rose to move to the right. In the second row, a larger force  $f_2 = (2.0, 0.0, 0.0)$  is applied in the same direction, resulting in more intense motion. This demonstrates that *Phys4DGen* can control the strength of motion by adjusting external force. In the third row, a leftward force  $f_3 = (-1.0, 0.0, 0.0)$ , with the same magnitude as in the first row, is applied along the x-axis. As a result, the orange rose moves left under this external force, demonstrating that *Phys4DGen* can control the direction of motion. To summarize, *Phys4DGen* allows fine-grained control of the dynamics in 4D content by adjusting external forces.

## 5. Conclusion

In this paper, we have introduced *Phys4DGen*, a novel, fast, physics-driven framework for generating 4D content from a single image. By integrating physical simulation directly into the 4D generation process, *Phys4DGen* ensures that the generated 4D content adheres to natural physical laws. Furthermore, we propose a Physical Perception Module (PPM) to infer the physical properties of different parts of 3D objects depicted in images, enabling more precise simulations and the generation of more physically realistic 4D content. To achieve controllable 4D generation, *Phys4DGen* incorporates external forces, allowing precise manipulation of the dynamics, such as movement speed and direction. Furthermore, by removing the need for iterative optimization in the 4D dynamics generation phase, *Phys4DGen* reduces 4D content generation time. Our extensive experiments show that *Phys4DGen* generates high-fidelity, physically accurate 4D content while significantly reducing generation time.



## References

- [1] Josh Achiam, Steven Adler, Sandhini Agarwal, Lama Ahmad, Ilge Akkaya, Florencia Leoni Aleman, Diogo Almeida, Janko Altenschmidt, Sam Altman, Shyamal Anadkat, et al. Gpt-4 technical report. *arXiv preprint arXiv:2303.08774*, 2023. 5
- [2] Sherwin Bahmani, Ivan Skorokhodov, Victor Rong, Gordon Wetzstein, Leonidas Guibas, Peter Wonka, Sergey Tulyakov, Jeong Joon Park, Andrea Tagliasacchi, and David B Lindell. 4d-fy: Text-to-4d generation using hybrid score distillation sampling. In *Proceedings of the IEEE/CVF Conference on Computer Vision and Pattern Recognition*, pages 7996–8006, 2024. 1, 2
- [3] Jason Bailey. The tools of generative art, from flash to neural networks. *Art in America*, 8:1, 2020. 1
- [4] Andreas Blattmann, Tim Dockhorn, Sumith Kulal, Daniel Mendelevitch, Maciej Kilian, Dominik Lorenz, Yam Levi, Zion English, Vikram Voleti, Adam Letts, et al. Stable video diffusion: Scaling latent video diffusion models to large datasets. *arXiv preprint arXiv:2311.15127*, 2023. 1
- [5] Junhao Cai, Yuji Yang, Weihao Yuan, Yisheng He, Zilong Dong, Liefeng Bo, Hui Cheng, and Qifeng Chen. Gaussian-informed continuum for physical property identification and simulation. *arXiv preprint arXiv:2406.14927*, 2024. 2
- [6] Ang Cao and Justin Johnson. Hexplane: A fast representation for dynamic scenes. In *Proceedings of the IEEE/CVF Conference on Computer Vision and Pattern Recognition*, pages 130–141, 2023. 2
- [7] Wen-Hsuan Chu, Lei Ke, and Katerina Fragkiadaki. Dreamscene4d: Dynamic multi-object scene generation from monocular videos. *arXiv preprint arXiv:2405.02280*, 2024. 2
- [8] Yutao Feng, Xiang Feng, Yintong Shang, Ying Jiang, Chang Yu, Zeshun Zong, Tianjia Shao, Hongzhi Wu, Kun Zhou, Chenfanfu Jiang, et al. Gaussian splashing: Dynamic fluid synthesis with gaussian splatting. *arXiv preprint arXiv:2401.15318*, 2024. 2
- [9] Quankai Gao, Qiangeng Xu, Zhe Cao, Ben Mildenhall, Wenchao Ma, Le Chen, Danhang Tang, and Ulrich Neumann. Gaussianflow: Splatting gaussian dynamics for 4d content creation. *arXiv preprint arXiv:2403.12365*, 2024. 2
- [10] Jonathan Ho, Ajay Jain, and Pieter Abbeel. Denoising diffusion probabilistic models. *Advances in neural information processing systems*, 33:6840–6851, 2020. 1
- [11] Tianyu Huang, Yihan Zeng, Hui Li, Wangmeng Zuo, and Rynson WH Lau. Dreamphysics: Learning physical properties of dynamic 3d gaussians with video diffusion priors. *arXiv preprint arXiv:2406.01476*, 2024. 3
- [12] Yanqin Jiang, Li Zhang, Jin Gao, Weimin Hu, and Yao Yao. Consistent4d: Consistent 360  $\{\deg\}$  dynamic object generation from monocular video. *arXiv preprint arXiv:2311.02848*, 2023. 2
- [13] Bernhard Kerbl, Georgios Kopanas, Thomas Leimkühler, and George Drettakis. 3d gaussian splatting for real-time radiance field rendering. *ACM Trans. Graph.*, 42(4):139–1, 2023. 2, 4
- [14] Justin Kerr, Chung Min Kim, Ken Goldberg, Angjoo Kanazawa, and Matthew Tancik. Lrf: Language embedded radiance fields. In *Proceedings of the IEEE/CVF International Conference on Computer Vision*, pages 19729–19739, 2023. 3
- [15] Alexander Kirillov, Eric Mintun, Nikhila Ravi, Hanzi Mao, Chloe Rolland, Laura Gustafson, Tete Xiao, Spencer Whitehead, Alexander C Berg, Wan-Yen Lo, et al. Segment anything. In *Proceedings of the IEEE/CVF International Conference on Computer Vision*, pages 4015–4026, 2023. 3, 4, 6
- [16] Hanwen Liang, Yuyang Yin, Dejia Xu, Hanxue Liang, Zhangyang Wang, Konstantinos N Plataniotis, Yao Zhao, and Yunchao Wei. Diffusion4d: Fast spatial-temporal consistent 4d generation via video diffusion models. *arXiv preprint arXiv:2405.16645*, 2024. 1, 2
- [17] Fangfu Liu, Hanyang Wang, Shunyu Yao, Shengjun Zhang, Jie Zhou, and Yueqi Duan. Physics3d: Learning physical properties of 3d gaussians via video diffusion. *arXiv preprint arXiv:2406.04338*, 2024. 3
- [18] Ben Mildenhall, Pratul P Srinivasan, Matthew Tancik, Jonathan T Barron, Ravi Ramamoorthi, and Ren Ng. Nerf: Representing scenes as neural radiance fields for view synthesis. *Communications of the ACM*, 65(1):99–106, 2021. 3
- [19] Zijie Pan, Zeyu Yang, Xiatian Zhu, and Li Zhang. Fast dynamic 3d object generation from a single-view video. *arXiv preprint arXiv:2401.08742*, 2024. 2
- [20] Minghan Qin, Wanhua Li, Jiawei Zhou, Haoqian Wang, and Hanspeter Pfister. Langsplat: 3d language gaussian splatting. In *Proceedings of the IEEE/CVF Conference on Computer Vision and Pattern Recognition*, pages 20051–20060, 2024. 3, 6
- [21] Ri-Zhao Qiu, Ge Yang, Weijia Zeng, and Xiaolong Wang. Feature splatting: Language-driven physics-based scene synthesis and editing. *arXiv preprint arXiv:2404.01223*, 2024. 3
- [22] Alec Radford, Jong Wook Kim, Chris Hallacy, Aditya Ramesh, Gabriel Goh, Sandhini Agarwal, Girish Sastry, Amanda Askell, Pamela Mishkin, Jack Clark, et al. Learning transferable visual models from natural language supervision. In *International conference on machine learning*, pages 8748–8763. PMLR, 2021. 3, 8
- [23] Jiawei Ren, Liang Pan, Jiayang Tang, Chi Zhang, Ang Cao, Gang Zeng, and Ziwei Liu. Dreamgaussian4d: Generative 4d gaussian splatting. *arXiv preprint arXiv:2312.17142*, 2023. 1, 2, 6
- [24] Robin Rombach, Andreas Blattmann, Dominik Lorenz, Patrick Esser, and Björn Ommer. High-resolution image synthesis with latent diffusion models. In *Proceedings of the IEEE/CVF conference on computer vision and pattern recognition*, pages 10684–10695, 2022. 1
- [25] Uriel Singer, Shelly Sheynin, Adam Polyak, Oron Ashual, Iurii Makarov, Filippos Kokkinos, Naman Goyal, Andrea Vedaldi, Devi Parikh, Justin Johnson, et al. Text-to-4d dynamic scene generation. *arXiv preprint arXiv:2301.11280*, 2023. 2

- [26] Jiaming Song, Chenlin Meng, and Stefano Ermon. Denoising diffusion implicit models. *arXiv preprint arXiv:2010.02502*, 2020. [2](#)
- [27] Qi Sun, Zhiyang Guo, Ziyu Wan, Jing Nathan Yan, Shengming Yin, Wengang Zhou, Jing Liao, and Houqiang Li. Eg4d: Explicit generation of 4d object without score distillation. *arXiv preprint arXiv:2405.18132*, 2024. [2](#)
- [28] Jiaxiang Tang, Jiawei Ren, Hang Zhou, Ziwei Liu, and Gang Zeng. Dreamgaussian: Generative gaussian splatting for efficient 3d content creation. *arXiv preprint arXiv:2309.16653*, 2023. [4](#)
- [29] Jiaxiang Tang, Zhaoxi Chen, Xiaokang Chen, Tengfei Wang, Gang Zeng, and Ziwei Liu. Lgm: Large multi-view gaussian model for high-resolution 3d content creation. *arXiv preprint arXiv:2402.05054*, 2024. [4](#), [6](#)
- [30] Yaohui Wang, Xinyuan Chen, Xin Ma, Shangchen Zhou, Ziqi Huang, Yi Wang, Ceyuan Yang, Yinan He, Jiashuo Yu, Peiqing Yang, et al. Lavie: High-quality video generation with cascaded latent diffusion models. *arXiv preprint arXiv:2309.15103*, 2023. [1](#)
- [31] Tianyi Xie, Zeshun Zong, Yuxing Qiu, Xuan Li, Yutao Feng, Yin Yang, and Chenfanfu Jiang. Physgaussian: Physics-integrated 3d gaussians for generative dynamics. In *Proceedings of the IEEE/CVF Conference on Computer Vision and Pattern Recognition*, pages 4389–4398, 2024. [2](#), [4](#), [5](#), [6](#)
- [32] Ziyi Yang, Xinyu Gao, Wen Zhou, Shaohui Jiao, Yuqing Zhang, and Xiaogang Jin. Deformable 3d gaussians for high-fidelity monocular dynamic scene reconstruction. In *Proceedings of the IEEE/CVF Conference on Computer Vision and Pattern Recognition*, pages 20331–20341, 2024. [1](#)
- [33] Mingqiao Ye, Martin Danelljan, Fisher Yu, and Lei Ke. Gaussian grouping: Segment and edit anything in 3d scenes. In *European Conference on Computer Vision*, pages 162–179. Springer, 2025. [3](#)
- [34] Yuyang Yin, Dejjia Xu, Zhangyang Wang, Yao Zhao, and Yunchao Wei. 4dgen: Grounded 4d content generation with spatial-temporal consistency. *arXiv preprint arXiv:2312.17225*, 2023. [1](#), [2](#)
- [35] Yifei Zeng, Yanqin Jiang, Siyu Zhu, Yuanxun Lu, Youtian Lin, Hao Zhu, Weiming Hu, Xun Cao, and Yao Yao. Stag4d: Spatial-temporal anchored generative 4d gaussians. *arXiv preprint arXiv:2403.14939*, 2024. [1](#), [2](#), [6](#)
- [36] Albert J Zhai, Yuan Shen, Emily Y Chen, Gloria X Wang, Xinlei Wang, Sheng Wang, Kaiyu Guan, and Shenlong Wang. Physical property understanding from language-embedded feature fields. In *Proceedings of the IEEE/CVF Conference on Computer Vision and Pattern Recognition*, pages 28296–28305, 2024. [3](#)
- [37] Lvmin Zhang, Anyi Rao, and Maneesh Agrawala. Adding conditional control to text-to-image diffusion models. In *Proceedings of the IEEE/CVF International Conference on Computer Vision*, pages 3836–3847, 2023. [1](#)
- [38] Tianyuan Zhang, Hong-Xing Yu, Rundi Wu, Brandon Y Feng, Changxi Zheng, Noah Snively, Jiajun Wu, and William T Freeman. Physdreamer: Physics-based interaction with 3d objects via video generation. *arXiv preprint arXiv:2404.13026*, 2024. [2](#)
- [39] Yuyang Zhao, Zhiwen Yan, Enze Xie, Lanqing Hong, Zhen-guo Li, and Gim Hee Lee. Animate124: Animating one image to 4d dynamic scene. *arXiv preprint arXiv:2311.14603*, 2023. [1](#), [2](#), [6](#)
- [40] Yufeng Zheng, Xueting Li, Koki Nagano, Sifei Liu, Otmar Hilliges, and Shalini De Mello. A unified approach for text-and image-guided 4d scene generation. In *Proceedings of the IEEE/CVF Conference on Computer Vision and Pattern Recognition*, pages 7300–7309, 2024. [2](#)
- [41] Licheng Zhong, Hong-Xing Yu, Jiajun Wu, and Yunzhu Li. Reconstruction and simulation of elastic objects with spring-mass 3d gaussians. *arXiv preprint arXiv:2403.09434*, 2024. [2](#)
- [42] Shijie Zhou, Haoran Chang, Sicheng Jiang, Zhiwen Fan, Zehao Zhu, Dejjia Xu, Pradyumna Chari, Suyu You, Zhangyang Wang, and Achuta Kadambi. Feature 3dgs: Supercharging 3d gaussian splatting to enable distilled feature fields. In *Proceedings of the IEEE/CVF Conference on Computer Vision and Pattern Recognition*, pages 21676–21685, 2024. [3](#)